Journal of Hazardous Materials 168 (2009) 406–415

Contents lists available at ScienceDirect

Journal of Hazardous Materials

journal homepage: www.elsevier.com/locate/jhazmat

Immobilization of *Trichoderma viride* for enhanced methylene blue biosorption: Batch and column studies

Asma Saeed [a], Muhammad Iqbal [a,*], Saeed Iqbal Zafar [b]

[a] *Biotechnology Group, Centre for Environment Protection Studies, PCSIR Laboratories Complex, Ferozepur Road, Lahore 54600, Pakistan*
[b] *School of Biological Sciences, University of Punjab, Lahore 54590, Pakistan*

ARTICLE INFO

Article history:
Received 22 September 2008
Received in revised form 16 January 2009
Accepted 9 February 2009
Available online 21 February 2009

Keywords:
Dye sorption
Immobilization
Loofa sponge
Trichoderma viride
Fixed-bed column
Methylene blue

ABSTRACT

An efficient dye biosorbent was developed by entrapping a fungus mold, *Trichoderma viride*, within loofa sponge (LS) matirx. Immobilization enhanced the sorption of dye by 30% at equilibrium as compared with *T. viride* free biomass (TVFB). The maximum dye biosorption capacity of *T. viride* immobilized onto loofa sponge (TVILS) and TVFB was found to be 201.52 and 155.06 mg g^{-1} biomass, respectively. The kinetics of dye removal by TVILS was rapid, with 84.3% sorption within the first 30 min and equilibrium after 90 min, whereas sorption by TVFB was slower as 61.4% dye was removed in first 30 min and equilibrium was achieved in 120 min. Biosorption kinetics and equilibria followed the pseudo-second-order and Langmuir adsorption models. FTIR spectroscopy of *T. viride* biomass showed that amine, hydroxyl, carbonyl and amide bonds were involved in the sorption of dye. Dye desorption from dye-laden TVILS with 0.1 M HCl was 99%. Regenerated TVILS was reusable without any appreciable decrease in its biosorption capacity during five repeated cycles. The dye removing capacity of TVILS in a continuous-flow column bioreactor was better than in batch-scale procedures. The study shows that TVILS has the potential of application as an efficient biosorbent for the removal of methylene blue from aqueous solutions.

1. Introduction

Synthetic dyes are released into the environment through industrial effluents [1]. Effluents containing synthetic dyes are hazardous to ecological systems and public health [2,3]. Due to these concerns, the removal of dyes from wastewaters has received considerable attention [4]. Treatment of dye-containing effluents is currently based on a variety of physicochemical procedures [5], which are usually inefficient, costly, and little adaptable to a wide range of dye wastewaters [6]. These inadequacies of the currently used procedures have led to studies on alternative methods that may be applied more efficiently and effectively.

Several investigations have focussed on biosorption of dyes by microorganisms, such as algae [7], fungi [8], bacteria [9] and yeasts [10]. Fungal biomass, among these, has been projected as efficient and inexpensive sorbent that can be produced at low-cost [11], or is available as waste from various industrial processes [12]. The use of fungal biomass for the remediation of dye effluents on a practical scale, however, has been hindered by operational limitations associated with their physical characteristics, such as small particle size with low density, poor mechanical strength and low rigidity, and the solid–liquid phase separation [13]. A further problem is associated with fragmentation of the hyphal biomass and cell mass sedimentation causing flow restrictions in the continuous-flow contact vessels. This has led to interest in the use of entrapped biomass as immobilized biosorption systems. Several immobilization media, such as sodium alginates and polysulfone [14], carboxymethylcellulose [15], and polyvinyl alcohol [16] have been used for the purpose. Due to their closed embedding structures, the immobilization matrices based on these polymeric gels, however, may cause mass transfer resistance resulting in restricted dye diffusion [13]. Their use is further limited by their insufficient mechanical strength and the lack of open spaces to accommodate active cell growth resulting in their rupture and cell release into the growth medium [17]. These problems were overcome by the application of fibrous network of loofa sponge (LS) and papaya wood in a novel procedure of fungal hyphae immobilization [18,19]. The biostructural matrix of these plant materials has extensive surface area, depressions and cavities making it ideally suited for immobilization of fungal hyphae. Whereas fungal biomass immobilized on loofa sponge has been used for the removal of heavy metals [20,21], its application for dye sorption is limited to only one preliminary report [22]. The potential shown in the study is extended to another dye and another fungus to elucidate the biosorption phenomenon in greater details. The present study thus reports for the first time the use of loofa sponge as immobilizing matrix to entrap *Trichoderma viride* as a low-cost biosorbent system for the removal of methylene blue from

* Corresponding author. Tel.: +92 42 9230688; fax: +92 42 9230705.
E-mail addresses: iqbalm@fulbrightweb.org, iqbalmdr@brain.net.pk (M. Iqbal).

0304-3894/$ – see front matter © 2009 Elsevier B.V. All rights reserved.
doi:10.1016/j.jhazmat.2009.02.058

aqueous solution. As best known to the authors, no earlier study reports using *T. viride* as a biosorbent of dyes. Besides exploring the dye biosorption potential of *T. viride* for the first time, the other significant aspect of the study relates to the development of an immobilized system that provides sufficient mechanical strength and stability to the biosorbent fungus, eliminates the laborious step of solid–liquid phase separation of free suspended biomass, and reports on the possibility of its reuse in repeated cycles. Methylene blue was selected as the adsorbate dye, which has been extensively studied earlier in several kinds of biosorption systems [4] and is one of the most important and widely used cationic dye in the textile and paper industries [13].

2. Materials and methods

2.1. Microorganism and culture medium

The microbial biomass used for dye biosorption in the present study was the fungus mold, *T. viride* (accession # 0142), obtained from the First Fungal Culture Bank of Pakistan, Department of Mycology and Plant Pathology, University of Punjab, Lahore, Pakistan, and maintained on malt extract agar slants. Subculturing of the stock culture slants was routinely done, every 4 weeks, incubated for growth at 30 °C for 5–7 d, later stored at 4 °C. Inoculum from these slants was used for the production of stationary phase hyphal suspension, free hyphal biomass, and fungal immobilization in liquid culture medium containing, per litre distilled water, 10 g glucose, 3 g $(NH_4)_2SO_4$, 0.3 g $MgSO_4{\cdot}7H_2O$, 0.1 g KCl, 0.05 g $CaCl_2$, 1 mg $FeCl_3$, and 0.1 g yeast extract. pH of the culture medium was adjusted at 6.0 ± 0.1.

2.2. Immobilizing material and technique

The loofa sponge (LS), obtained from matured dried fruit of *Luffa cylindrica*, was used for the immobilization of *T. viride*. Immobilization of *T. viride* within the fibrous network of LS was carried out following the procedure reported in detail earlier [18]. The LS was cut into discs of approx 2.4–2.5 cm and 2–3 mm thickness (Fig. 1a), soaked in boiling water for 30 min, thoroughly washed under tapwater, and left for 24 h in distilled water, changed 3–4 times. The LS discs were oven-dried at 70 °C and stored in desiccator till further use. The procedure of hyphal biomass immobilization of *T. viride* within the LS discs is briefly summarized below. Four pre-weighed LS discs were transferred to 250-mL Erlenmeyer flasks containing 100 mL of the liquid culture medium, autoclaved, and on cooling inoculated with 0.5 mL of stationary phase hyphal suspension of *T. viride*. Similar procedure, but without the LS discs, was followed

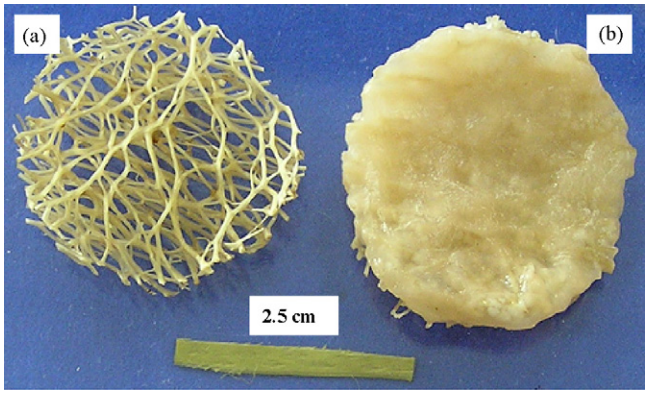

Fig. 1. Immobilization of *Trichoderma viride* within the loofa sponge of *Luffa cylindrica*: (a) raw loofa sponge disc; (b) loofa sponge disc covered with immobilized hyphal biomass of *T. viride*.

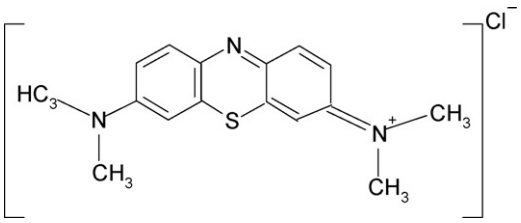

Fig. 2. Chemical structure of methylene blue.

for the production of free hyphal biomass. The inoculated cultures were incubated at 35 °C, shaken at 100 rpm for 7 d. The incubated cultures were harvested as *T. viride* free hyphal biomass (TVFB) and *T. viride* immobilized onto loofa sponge (TVILS) discs, washed twice with distilled water, and freeze dried. Dry weight of *T. viride* hyphal biomass entrapped within the LS discs was determined as the weight difference of LS discs before and after *T. viride* biomass immobilization procedure.

2.3. Dye solution preparation

Methylene blue (C.I. #52015, also called Basic Blue 9, molecular weight: 373.91, λ_{max} 665 nm) was obtained from E. Merck, Darmstadt, Germany. The chemical formula of methylene blue (MB) is $C_{16}H_{18}N_3SCl.3H_2O$ (3,7-bis[dimethylamine]-phanazathionium chloride; tetramethylthionine chloride), with the aromatic moiety planar having the dimethyl amino groups attached to the aromatic unit (Fig. 2). MB is a water-soluble cationic dye, though usually categorized as basic dye. The cationic character of the MB molecule originates from the positive charge of N or S atoms, which is generally delocalized throughout the chromophoric system, although it is probably more localized on the N atoms [23]. MB solution was prepared by diluting 1.0 g L^{-1} dye, which was obtained by dissolving weighed quantity of MB in double-distilled water. Fresh dye solutions of the desired dye concentrations were made at the start of each experiment.

2.4. Biosorption procedure for equilibrium and kinetics studies

The biosorption capacity of exact hyphal biomass of TVFB and TVILS (100 mg) was determined by contacting 100 mL MB solution of known concentrations (10–800 mg L^{-1}) in 250-mL Erlenmeyer flasks. The dye solution, incubated with the biosorbent (TVFB; TVILS), was shaken on an orbital shaker at 100 rpm in tightly stoppered flasks at ambient temperature (30 ± 2 °C) for 2 h to ensure equilibrium. TVFB was removed from the dye solution by centrifugation at 5000 rpm for 5 min, whereas TVILS discs were separated from the solution by simple decantation. Residual concentration of the dye supernatant solution was determined spectrophotometerically (Hitachi 220 UV/VIS spectrophotometer) at 665 nm. Dilutions were made when absorbance exceeded 1.5. The effect of pH was determined by varying dye solution pH in the range of 2–10. Dye-free solution (double-distilled water) and TVILS-free dye solution containing only LS disc blanks were used as controls. The effect of temperature on biosorption was determined at 10 °C intervals for the range of 20–50 °C. For determining the optimum time for biosorption equilibrium and kinetics of biosorption, the sorbate-sorbent contact was continued for several time periods ranging between 15 min and 6 h.

2.5. Desorption and reuse of regenerated biosorbents

The MB-loaded biomass of both TVFB and TVILS, which was initially exposed to 100 mg l^{-1} of MB at pH 7.0 and 30 °C, was contacted with 50 mL of 0.1 M HCl as the dye-desorbing agent for 120 min on

a rotary shaker at 100 rpm. After desorption, the TVFB and TVILS biosorbents were washed several times with double-distilled water and the regenerated biosorbents were reused for the next cycle following the same procedure as employed in the biosorption equilibrium experiments. These cycles of biosorption–desorption were repeated five times.

2.6. Continuous removal of MB by TVILS packed in fixed-bed columns

A glass column (2.7 cm in diameter and 35 cm in height) was packed with LS discs containing 2.56 ± 0.14 g of immobilized biomass of *T. viride* (TVILS), packing height 30 cm. Dye solution (25 mg L^{-1}, pH 7.0) was then pumped upwards through the column at a flow rate of 2.5 mL min^{-1}. Samples were collected at regular intervals from the effluent to measure residual dye concentrations. As the bed was saturated, the dye loading was terminated and the bed was eluted with 0.1 M HCl solution to recover the loaded dye. The regenerated bed was washed thoroughly with deionized water before use in the next fixed-bed adsorption column cycle.

2.7. FTIR spectroscopy

Preliminary detection of the chemical functional groups present in the hyphae of *T. viride*, before and after MB loading, for determining their possible involvement in the dye biosorption process, Fourier transform infrared (FTIR) spectroscopic analysis was done in solid phase. IR absorbance data were obtained for the wavenumber range of 500–4000 cm^{-1} using Thermo-Nicolet IR-100 spectrometer (Thermo-Nicole Corporation, Madison, USA). Data analysis was done on Encompass® software provided by the FTIR spectrometer manufacturer. For obtaining FTIR spectra, ball-milled fungal hyphae biomass was mixed with KBr (ratio 1:100), compacted into a tablet form using a bench press, and the material was run for obtaining FTIR spectra.

2.8. Reproducibility and data analysis

Unless indicated otherwise, the data reported are the mean values of three separate experiments. The amount of dye adsorbed per unit free and immobilized hyphal biomass (mg dye g^{-1} dry biosorbent) was determined using the following expression:

$$q = \frac{V(C_i - C)}{M} \quad (1)$$

where q is the dye uptake (mg dye g^{-1} dry weight of the hyphal biomass, free or entrapped within LS), V is the volume of dye solution (L), C_i is the initial concentration of dye in the solution (mg L^{-1}), C is the residual concentration of dye in the solution at any time, and M is the dry weight of hyphal biomass (g).

The Langmuir and Fruendlich equilibrium models [24,25] were used for evaluation of the adsorption data. Langmuir isotherm assumes monolayer adsorption, and is presented by the following equation:

$$q_{eq} = \frac{q_{max} b C_{eq}}{(1 + bC_{eq})} \quad (2)$$

where q_{eq} and q_{max} are, respectively, the equilibrium and maximum dye uptake capacities (mg g^{-1} biosorbent), C_{eq} is the equilibrium dye concentration (mg L^{-1} solution), and b is the Langmuir equilibrium constant (L mg^{-1}).

The Freundlich model is presented as below:

$$q_{eq} = K_F C_{eq}^{1/n} \quad (3)$$

where K_F and n are the Freundlich constants characteristic of the system.

In order to examine the controlling mechanism of the biosorption process, such as mass transfer and chemical reaction, the pseudo-first-order and the pseudo-second-order kinetics models, were used to test the experimental data of dye biosorption by TVILS and TVFB. The pseudo-first-order rate equation of Lagergren [26] is presented as:

$$\ln(q_{eq} - q_t) = \ln q_{eq} - k_{1ad} t \quad (4)$$

where q_{eq} (mg g^{-1}) is the mass of dye adsorbed at equilibrium, q_t (mg g^{-1}) is the mass of dye adsorbed at time t, and k_{1ad} (min^{-1}) is the pseudo-first-order reaction rate constant. The pseudo-first-order considers the rate of occupation of adsorption sites to be proportional to the number of unoccupied sites. A straight line of $\ln(q_{eq} - q_t)$ versus t indicates the application of the pseudo-first-order kinetics model. In a true pseudo-first-order process, $\ln q_{eq}$ should be equal to the intercept of a plot of $\ln(q_{eq} - q_t)$ against t.

In addition, a pseudo-second-order equation [27], based on adsorption equilibrium capacity, may be expressed in the following form:

$$\frac{t}{q_t} = \frac{1}{k_{2ad} q_{eq}^2} + \frac{1}{q_{eq}} t \quad (5)$$

where k_{2ad} (g mg^{-1} min^{-1}) is the pseudo-second-order reaction rate equilibrium constant. A plot of t/q_t against t should give a linear relationship for the applicability of the pseudo-second-order kinetics model.

Eqs. (4) and (5) can be transformed into non-linear forms, as given in Eqs. (6) and (7). These can then be used to predict the adsorption equilibrium and kinetics rate constants:

$$q_t = q_{eq}[1 - \exp(-k_{1ads} t)] \quad (6)$$

$$q_t = \frac{q^2 k_{2ad} t}{1 + q_{eq} k_{2ad} t} \quad (7)$$

In order to evaluate the error of model predictions, the root mean square errors (RMSE) were calculated for kinetics models. The sum of the square of the difference between the dye removal experimental data (q), and model predictions (q_m) was divided by the number of data points (p) for each data set, and the square root of this term was taken:

$$\mathrm{RMSE} = \sqrt{\frac{\sum_{1}^{p} (q - q_m)^2}{p}}$$

3. Results and discussion

3.1. T. viride loading on LS to produce TVILS discs

Physical examination of the LS discs revealed hyphal growth in the sponge matrix within 24 h of incubation. Complete coverage of the LS discs with hyphae of *T. viride* occurred within 5 d. However, biomass accumulation/loading was noted to continue until the attainment of stationary phase of growth upto 7 d. No free hyphal growth was observed in the immobilization system (TVILS) during this period and the LS discs appeared as compact units of fungal biomass (Fig. 1b).

3.2. FTIR spectroscopic detection of functional groups in T. viride

The pattern of adsorption is relatable to the active groups and bonds present in the biosorbent material [28]. For the detection

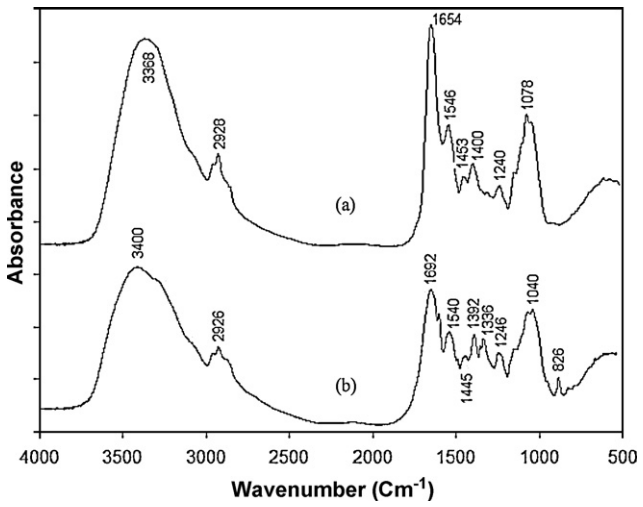

Fig. 3. Fourier transform infrared (FTIR) spectra of *Trichoderma viride*: (a) before and (b) after biosorption of methylene blue.

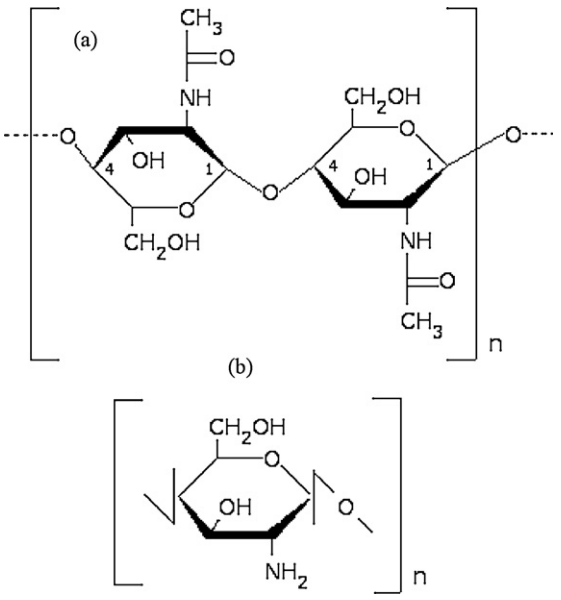

Fig. 4. Structure of chitin molecule: (a) showing two of the *N*-acetyl-β-D-glucosamine units that repeat to form long chains of β-1,4 linkage, and (b) a repeating unit of β-D-glucosamine.

of active biosorption sites, therefore, FTIR spectra of the virgin and MB-adsorbed *T. viride* hyphae were obtained (Fig. 3). Peaks appearing in the FTIR spectra were assigned to various groups and bonds in accordance with their respective wavenumbers (cm^{-1}) as reported in literature for other fungi, such as *Aspergillus niger*, *Phanerochaete chrysosporium* and *Lentinus sajor-caju* [29–31]. The three most prominent peaks in the virgin hyphae were observed at 3368, 1654 and 1078 cm^{-1} (Fig. 3a). The peak at 3368 cm^{-1} was stronger and broad due to amine group stretching vibrations superimposed on the side of hydroxyl group band, which has been reported to occur at 3500–3300 cm^{-1} [30]. The peak at 2928 cm^{-1} is indicative of C–H bond [28]. The strong peak at 1654 cm^{-1} and the two peaks at 1400 and 1240 cm^{-1} were caused by C=O stretching mode of carboxyl group conjugated to a –NH deformation mode resulting in –CO–NH–, indicative of amide bond formation [17]. The peak at 1546 cm^{-1} represents amine group stretching vibration resulting from –NH deformation mode conjugated to C=N deformation mode. The phosphate groups showed the characteristic peak at 1078 cm^{-1} representing P–OH stretching [30]. The functional groups detected in the FTIR spectrum relate well with the chemical structure of chitin, which is a specific constituent of fungus cell walls [32]. Chitin is a polysaccharide of repeating units of *N*-acetyl-β-D-glucosamine covalently linked by β-1,4 bonds similar to the linkages between glucose units forming cellulose, and also containing a small number of β-D-glucosamine units in the chitin polymeric chain (Fig. 4). Chitin is thus essentially a cellulose polymer with one –OH group on each monomer substituted with an acetylamine group. The FTIR spectrum of *T. viride* hyphae loaded with MB showed shifts of several peaks when compared with the FTIR spectrum of virgin *T. viride* hyphae (Fig. 3a and b). However, most significant shifts in the FTIR spectrum peaks of the virgin *T. viride* hyphae were noted from 3368 cm^{-1} (amine group superimposed on hydroxyl group), and 1654 and 1240 cm^{-1} (carboxyl group conjugated to a –NH deformation mode forming the amide group –CO–NH–), respectively, to 3400, 1692 and 1246 cm^{-1} in the *T. viride* hyphae loaded with MB, indicating that amine, hydroxyl, carbonyl and amide bonds were the major sites for sorption of the cationic dye. The involvement of other functional sites detected in the FTIR spectrum of the virgin *T. viride* may be rated as minor. The functional groups detected in the virgin *T. viride* hyphae, and are likely involved in the biosorption of MB, have been also reported to occur in chitin, which is known to be an effective dye adsorbent [33].

3.3. Effect of pH on biosorption

Previous studies have reported that solution pH is among the most significant parameters controlling the sorption of MB [34]. This is possibly due to its impact on both the surface binding sites of the biosorbent and ionization status of the dye molecule in water [35]. Since dye adsorption can dramatically change with the change of solution pH, it has been stressed that not only should it be accurately reported but also data for all comparative studies must be obtained at the same pH values [36]. Therefore, the impact of pH on the biosorption of MB by LS, TVFB and TVILS discs was studied in the range between 2 and 10 to determine the optimum pH value for dye adsorption. Appropriate pH of the sorbent-sorbate system was adjusted by adding 1 M NaOH or HCl. The MB molecule on dissolution in water releases coloured dye cations, which are electrostatically attracted towards the negatively charged biosorbent surface [37,38]. The biosorption of these positively charged dye cations is primarily influenced by the degree of negative surface charge on the adsorbent, which is essentially determined by the solution pH. Such a consideration has been well shown in the present studies by the effect of solution pH in the range of 2–10 on removal of MB by the two variants of *T. viride* used as biosorbents. It may be noted from Fig. 5, accordingly, that MB biosorption from 100 mg l^{-1} dye solution by TVFB and TVILS, after 120 min of contact, was minimal at pH 2 (17.43 and 27.09 mg g^{-1}), which significantly increased respectively to 69.07 and 85.62 mg g^{-1} at pH 6, and 71.82 and 87.37 mg g^{-1} at pH 7. Further increase from pH 7 to 10 showed unchanged MB adsorption plateau. These results have shown that availability of negatively charged groups at the adsorbent surface is necessary for adsorption of the cationic dye to proceed. At low pH, the availability of negatively charged adsorbent sites is expected to be low due to the presence of excess H^+ ions competing with dye cations for adsorption sites [39] as there is a net positive charge in the adsorption system due to the presence of H_3O^+. It has been concluded that in such a system, H^+ ions compete with the dye cations, resulting in active sites getting protonated to the exclusion of dye cations binding on the adsorbent surface [1]. Also, at lower pH, the number of negatively charged sites is low, which is not favourable for the adsorption of positively charged dye cations due to electrostatic repulsion [40]. As pH of the dye solution

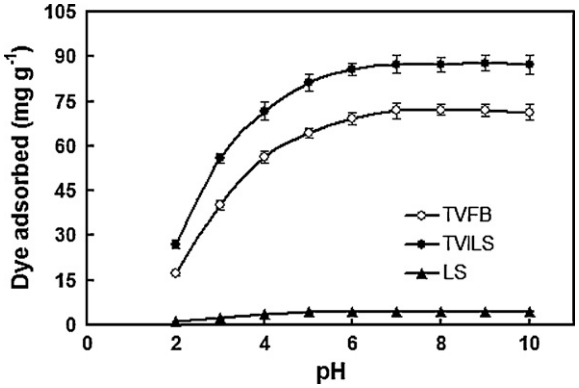

Fig. 5. Effect of pH on the sorption capacities of loofa sponge (LS), *Trichoderma viride* free biomass (TVFB) and *T. viride* immobilized onto loofa sponge (TVILS) for the removal of methylene blue from 100 mL of 100 mg L^{-1} dye solution during orbital shaking at 100 rpm for 120 min and 30 °C.

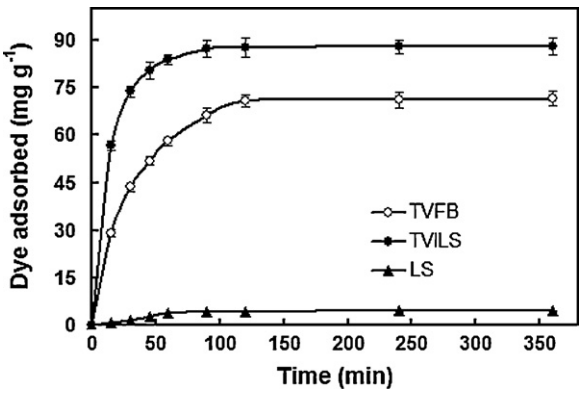

Fig. 7. Effect of incubation time on the sorption capacities of loofa sponge (LS), *Trichoderma viride* free biomass (TVFB) and *T. viride* immobilized onto loofa sponge (TVILS) on the removal of methylene blue from 100 mL of 100 mg L^{-1} dye solution, pH 7.0, on orbital shaking at 100 rpm and 30 °C.

was increased, more negatively charged surface sites became available due to deprotonation of different functional groups present on the biosorbent (see Section 3.2). This resulted in an increase in the electrostatic force between the negatively charged biosorbent and positively charged MB ions, thus resulting in increased MB adsorption. Similar trends, where the biosorbent surface was negatively charged, were observed for MB sorption, such as on *Fomes fomentarius* and *Phellinus igniarius* [12], *Corynebacterium glutamicum* [41], and various carbon adsorbents [42].

3.4. Effect of temperature on dye biosorption

Effect of temperature on the biosorption of MB by TVFB and TVILS at equilibrium was investigated at the temperature intervals of 10 °C in the range between 20 and 50 °C, at the initial dye concentration of 100 mg L^{-1}, pH 7.0 (Fig. 6). The biosorption of MB was noted to enhance with the increase in temperature upto 50 °C indicating that higher temperature favoured the removal of dye by sorption onto both TVFB and LIBTV. The observation is in agreement with an earlier report on the biosorption of Acid Blue 161 by *Trametes versicolor* [43]. The enhanced adsorption at higher temperatures was suggested to be due to increase in the availability of active surface sites, increased porosity, and in the total pore volume of the adsorbent. These authors further suggested that the enhancement in adsorption may also be a result of an increase in the mobility of the dye molecule with an increase in their kinetic energy, enhanced rate of intraparticulate diffusion of the sorbate

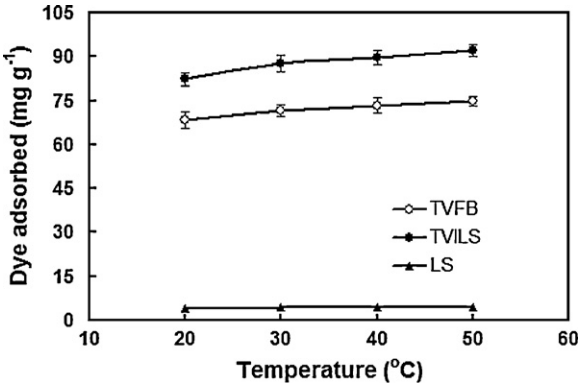

Fig. 6. Effect of temperature on the equilibrium sorption capacity of loofa sponge (LS), *Trichoderma viride* free biomass (TVFB) and *T. viride* immobilized onto loofa sponge (TVILS) on the removal of methylene blue from 100 mL of 100 mg L^{-1} dye solution at pH 7.0, on orbital shaking for 120 min at 100 rpm.

dye, and due to decrease in thickness of the boundary layer surrounding the sorbate dye at a higher temperature so that the mass transfer resistance of the sorbate in the boundary layer decreases [43]. The observations on the biosorption of MB sorbate on both TVFB and TVILS disc sorbents in the present study further suggest that it was an endothermic process and may involve not only physical but also chemical sorption, as suggested in an earlier study on the biosorption of Remazol Black B by *Rhizopus arrhizus* [44].

3.5. Effect of contact time

In order to determine the effect of contact time on the dye binding capacity of TVFB and TVILS, both biosorbents were contacted with 100 mg L^{-1} aqueous MB dye solution for various intervals ranging between 15 min and 6 h at pH 7.0 and 30 °C temperature. The rate of dye uptake by TVILS was rapid, with the maximum uptake achieved in the first 30 min amounting to 84.3% sorption (Fig. 7). The sorption rate after this initial fast phase, however, was observed to slow down significantly until it reached a plateau after 90 min, indicating equilibrium of the system. In comparison, maximum uptake of MB by TVFB in the first 30 min was 61.4%, while the equilibrium was established in 120 min. It was also noted that after the adsorption equilibrium time of 90 and 120 min of TVILS and TVFB, respectively, no further dye adsorption took place suggesting that the active sites available on the biosorbent surface were the limiting factor. It is significant to point out that at each stage of time interval, the dye removal by TVILS was appreciably higher than by TVFB, thus clearly showing the superiority of TVILS over TVFB as the biosorbent. The significant lower uptake of MB by TVFB may be attributed to the hyphal aggregation due to electrostatic interaction in the form of pellets, thus reducing the surface area and blocking access of the dye to active sites of sorption. The higher sorption of MB by TVILS, on the other hand, is evidently due to the expanded surface area of the immobilized fungal hyphae along the fibrous structure of the LS, and the open structure of TVILS provided by the LS biostructural matrix, which together enhance free access of the dye to sorption sites. The rapid rate of MB sorption by TVILS observed during the present study has a significant practical importance for applications in small reactor volumes, thus ensuring efficiency and economy. This is a significant advantage over other immobilized biosorbents reported previously for both dye and metal biosorption. For example, fungal biomass of *Corynebacterium glutamicum* immobilized in polysulfone and alginate removed Reactive Black 5 dye slowly, achieving equilibrium in 300 and 450 min, which was respectively 66% and 150% higher than the time taken by free biomass (180 min) in the same study

[14]. Similarly, yeast biomass immobilized in polyvinyl alcohol and alginate was reported to remove metal ions very slowly, achieving equilibrium in 12 and 24 h, respectively, which was about 24 and 48 times greater than the time taken by free yeast biomass (30 min) in the same study [45]. In another study, microbial biomass immobilized in sodium alginate beads took 15 h to reach equilibrium for the removal of Cd(II), which was 100 times more than the time taken by free cells [46]. The authors suggested that the observed slow rate of Cd(II) uptake by the microbial biomass immobilized in alginate beads was caused by restriction exerted on the diffusion of Cd(II) through the gel matrix. A slower rate of copper biosorption by hydrophilic polyurethane foam-immobilized biomass of *Ascophyllum nodosum* has been also reported [47]. The foam-immobilized biomass took about 320 min to achieve equilibrium as compared with less than 90 min needed by free biomass. The slower rate of metal adsorption by the immobilized biomass was suggested to be due to the additional time taken for the solute to diffuse through the foam membrane and reach the functional groups on the biomass surface. Arguments given for slow metal biosorption by biomass encapsulated in synthetic polymers is likewise applicable for dye removal, which being a large molecule is expected to encounter greater diffusion restriction than the small size of metal ions. In the case of TVILS, however, no such problem was presented due to the surface immobilization of fungal hyphae and the open-face solid–liquid phase contact provided by the highly porous biostructural matrix of LS and thus the process of biosorption was completed within 90 min. To ensure equilibrium, however, a contact time of 120 min was used for further studies on biosorption of MB by both TVFB and TVILS.

3.6. Dye removal capacity of TVILS and adsorption isotherms

Significant potential of dye removal from aqueous solution was demonstrated by TVILS. The maximum dye biosorption capacity of TVILS was noted to be $201.52 \pm 4.63\ mg\ g^{-1}$, whereas the maximum removal of dye by TVFB was $155.06 \pm 5.27\ mg\ g^{-1}$ (Fig. 8). This indicates a 29.96% higher dye removal capacity of TVILS than TVFB. The removal of dye by LS discs without immobilized fungal hyphal biomass (naked LS) in the control run was found to be $13.11 \pm 0.43\ mg\ g^{-1}$. Though it is not possible to predict how much of it contributed to the $201.52 \pm 4.61\ mg\ g^{-1}$ dye biosorbed by the TVILS biosorbent system, yet most of it is likely to have been adsorbed on the expanded surface area of this unique biosorbent matrix provided by the fungal hyphal biomass immobilized along the outer surface of the fibrous structure of LS, which was completely covered by fungal hyphae (Fig. 1b) thus significantly masking the LS sorption sites. From these results, nevertheless, it is clear that the use of LS as an immobilization matrix has significantly enhanced the biosorption capacity of TVILS and has caused no negative effect on the biosorption process. This is a significant achievement in the development of immobilized biosorbent systems as most of the previously reported microbial immobilized biosorbents using synthetic polymers are known to have resulted in a significant decrease in dye uptake in comparison with free cell biomass used as biosorbents. For example, 28.85% decrease in the sorption of MB was noted when algal biomass was immobilized in polyacrylonitrile (PAN) as compared with free algal cell biomass [48]. Similarly, 19.89% and 17.33% reduction in the sorption of Reactive Black 5 was observed when biomass of *C. glutamicum* was immobilized, respectively, in alginate and polysulfone gel beads as compared with free cells [14], while another study reported 32.2% decrease in the uptake of the same dye when *C. glutamicum* cells were immobilized in polysulfone matrix as compared with free cell biomass [13]. Similar decrease in the biosorption capacity of immobilized biomass, as compared to free biomass has been reported for metal uptake also [49,50]. These reductions have been projected to be due to the limitations exerted in the movement of adsorbate, or masking of active sites on the biosorbent [14]. Moreover, part(s) of the cell surface might be shielded by the gel matrix, which would thus become unavailable for adsorbate binding [46]. In the present study, surface immobilization of *T. viride* on the biostructural fibrous network of LS discs enables a direct contact of the biomass to MB solution, which is thus well suited for biosorption than the enclosed or beaded immobilization systems based on polymeric gel matrices.

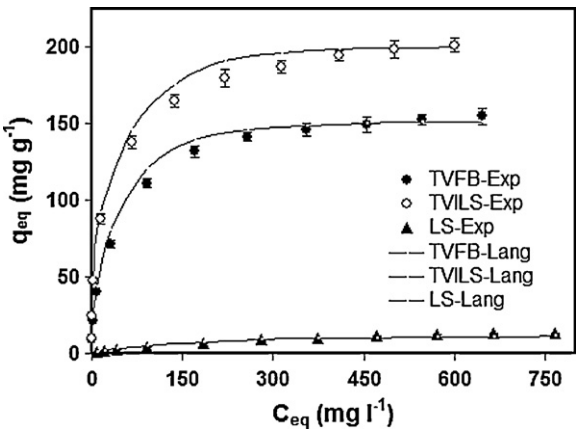

Fig. 8. Biosorption of methylene blue by loofa sponge (LS), *Trichoderma viride* free biomass (TVFB) and *T. viride* immobilized onto loofa sponge (TVILS) from 100 mL of the dye solution (10–800 mg L^{-1}, pH 7.0) on orbital shaking for 120 min at 100 rpm and 30 °C, where C_{eq} is the equilibrium dye concentration and q_{eq} is the dye adsorbed per unit biosorbent weight. Langmuir predictions are shown in solid curve.

Analysis of the equilibrium data is important for developing an equation for design purposes. Several isotherms equations have been used for the equilibrium modelling of biosorption systems. Out of these isotherms equations, the two that have been applied to the data obtained during the present study were the Freundlich and Langmuir isotherms. For each isotherm modelling, initial dye concentrations were varied (10–800 mg L^{-1}), whereas the TVILS weight in each sample was kept constant. The Langmuir and Freundlich adsorption constants, as determined from these isotherms, and their correlation coefficients are presented in Table 1. Very high regression correlation coefficients (>0.99) for Langmuir isotherms model were noted for both TVFB and TVILS, which show that this model was suitable for describing the biosorption equilibrium data of MB by fungal biomass in the studied concentrations range. The r^2 values in the case of Freundlich isotherms were relatively low, which were 0.954 and 0.946 for TVFB and TVILS, respectively. The

Table 1
Isotherms model constants and their respective correlation coefficients for biosorption of methylene blue from aqueous solution by *Trichoderma viride* free biomass (TVFB) and *T. viride* immobilized onto loofa sponge (TVILS).

Biosorbents	Experimental	Langmuir isotherm model			Freundlich isotherm model		
	q_{max} (mg g^{-1})	q_{max} (mg g^{-1})	b (L mg^{-1})	r^2	K_F	n	r^2
TVFB	155.06 ± 5.27	151.48	0.065	0.991	13.36	2.41	0.954
TVILS	201.52 ± 4.63	200.24	0.262	0.996	28.19	2.96	0.946

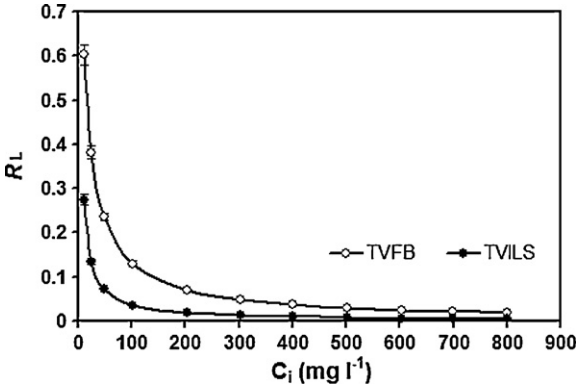

Fig. 9. Value of separation factor (R_L) for the sorption of methylene blue by *Trichoderma viride* free biomass (TVFB) and *T. viride* immobilized onto loofa sponge (TVILS), where C_i is the initial dye concentration.

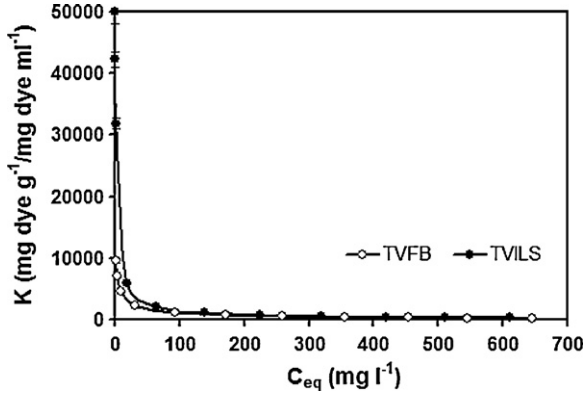

Fig. 10. Distribution coefficient of methylene blue biosorption by *Trichoderma viride* free biomass (TVFB) and *T. viride* immobilized onto loofa sponge (TVILS) where C_{eq} refers to dye concentration at equilibrium and K is adsorption distribution coefficient.

Langmuir parameters can also be used to predict affinity between the sorbate and the sorbent using the dimensionless separation factor (R_L), which has been defined as below [51]:

$$R_L = \frac{1}{1 + bC_0} \quad (6)$$

where R_L is the dimensionless separation factor, C_0 is the initial concentration of the adsorbate (mg L^{-1}), and b is the Langmuir constant (L mg^{-1}). The R_L value can be used to predict whether a sorption system is "favourable" or "unfavourable" [51,52]. If the average of the R_L values at different initial concentrations is between 0 and 1, it indicates favourable adsorption [48]. The R_L values for sorption of MB on TVFB and TVILS are shown in Fig. 9. The average values of R_L for the adsorption of MB onto TVFB and TVILS at different initial dye concentration as calculated from Fig. 9 are 0.234 and 0.146, respectively, indicating that the adsorption of dye by fungal biomass was a favourable process.

3.7. Distribution coefficient

The adsorption distribution coefficient (K), which is the ratio of equilibrium concentration in the solid and liquid phase, is shown in Fig. 10. A high value of distribution coefficient is characteristic of a good biosorbent. TVILS exhibited a K value of 49950 mL g^{-1} dry weight at C_{eq} of 0.21 mg MB L^{-1}, which was almost 5.21 times greater than the distribution coefficient value obtained for TVFB (9589.5 mL g^{-1} dry weight at C_{eq} of 4.12 mg MB L^{-1}). These results clearly indicate that TVILS, in addition to having higher biosorption rate and capacity (Table 1), also showed higher distribution value, which confirms the superiority of TVILS over TVFB.

3.8. Biosorption kinetics modelling

In order to analyze biosorption kinetics of MB, pseudo-first-order and pseudo-second-order kinetics models were applied to the biosorption data and non-linear fitting was performed to determine the model parameters. Fit to these models is shown in Fig. 11, whereas Table 2 summaries the rate constants (k) and equilibrium dye uptake (q_{eq}) as determined by non-linear parameter optimization for both TVFB and TVILS. Experimental data for the biosorption of MB by both TVFB and TVILS with average errors being only 1.34–2.25 mg g^{-1} and 1.33–1.98 mg g^{-1}, which correspond to 2–3% and 1.5–2% of q_{eq} for TVFB and TVILS, respectively, were noted to fit well to both the pseudo-first-order and pseudo-second-order kinetics models (Table 2). However, pseudo-first-order kinetics model seems to show slightly better fit for both the biosorbents when compared with pseudo-second-order model, since it presented the lower RMSE values, which meant that the fit of predicted q_{eq} values to pseudo-first-order model was closer to experimentally measured q_{eq} values for all the experimental points. These observations are in accordance with findings of other researchers, who have successfully employed the non-linear kinetics and equilibrium equations to obtain the adsorption parameters with excellent accuracy for different adsorbates and adsorbents [53–55]. The non-linear kinetics equations were preferred over linear equations, since the latter does not take into account the errors associated with each experimental point, which cannot always be linearized [56]. The pseudo-first-order model describes adsorption reactions at the

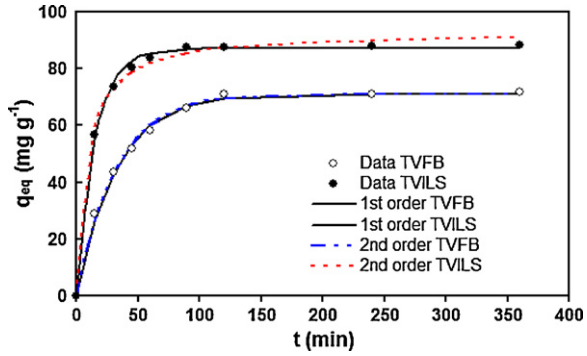

Fig. 11. Plots showing fit of experimental data to pseudo-first-order and pseudo-second-order kinetics models for the removal of methylene blue from aqueous solution using *Trichoderma viride* free biomass (TVFB) and *T. viride* immobilized onto loofa sponge (TVILS); conditions: initial MB concentration of 100 mg L^{-1}, pH 7.0, biosorbent dosage 1 g L^{-1} and temperature 30 °C.

Table 2
Theoretically determined constants of pseudo-first-order and pseudo-second-order reaction kinetics, calculated from non-linear equations, based on the sorption of methylene blue from 100 mL of 100 mg L^{-1} dye solutions, pH 7, by 1.0 g L^{-1} *Trichoderma viride* free biomass (TVFB) and *T. viride* immobilized onto loofa sponge (TVILS).

Biosorbent	Experimental q_{eq} (mg g^{-1})	Pseudo-first-order constants			Pseudo-second-order constants		
		q_{eq} (mg g^{-1})	k_{1ad} (min^{-1})	RMSE (mg g^{-1})	q_{eq} (mg g^{-1})	k_{2ad} (g mg^{-1} min^{-1})	RMSE (mg g^{-1})
TVFB	72.02 ± 2.29	71.2	0.031	1.34	79.9	0.00053	2.25
TVILS	88.20 ± 2.61	87.1	0.066	1.33	93.1	0.0013	1.98

Table 3
Biosorption and elution of methylene blue in repeated cycles by *Trichoderma viride* free biomass (TVFB) and *T. viride* immobilized onto loofa sponge (TVILS) in batch-scale studies carried out in 250-mL Erlenmeyer flasks.

Cycle no.	Biosorption (mg g^{-1})	Biosorption decline (%)	Elution (mg g^{-1})	Elution (%)	Loss in biomass weight (%)
Free biomass (TVFB)					
1st	72.83 ± 2.13		71.86 ± 3.08	98.67	
5th	58.47 ± 2.45	19.72.	57.92 ± 1.52	99.05	15.62
Immobilized biomass (TVILS)					
1st	88.15 ± 2.07		87.48 ± 2.76	99.23	
5th	84.25 ± 1.82	4.42	84.16 ± 3.21	99.09	3.98

particle–solution interface, and frequently shows biphasic kinetics with a fast rate at the beginning followed by a slower rate. Accordingly, the experimental data can be described by two phased pseudo-first-order reaction behaviour, which may be interpreted as reactions on two types of sites, namely, external sites that are quickly accessible and internal sites that are less accessible and show slower rates of sorption [57,58].

3.9. Desorption and reuse of TVILS

Reusability of a biosorbent is of critical significance in practical applications for dye removal from wastewaters. The capacity of TVILS to adsorb dye was, therefore, determined by repeated adsorption–desorption cycles. Since maximum biosorption of MB was noted to occur near neutral to basic conditions, it seems logical that the sorbed MB may be recovered under strong acidic conditions. Therefore, 0.1 M HCl was used as an elutant during the present studies. Under strong acidic conditions (pH < 1), the number of positively charged sites on the biosorbent surface are expected to favour desorption of the cationic MB dye due to electrostatic repulsion. Higher than 99% desorption of MB was obtained for both TVFB and TVILS. The TVILS used in successive adsorption–desorption cycles was noted to retain good MB adsorption capacity even after five cycles (Table 3). The total decrease in sorption efficiency of TVILS after five adsorption–desorption cycles was only about 4.3%, which shows that TVILS has good potential to adsorb the dye from aqueous solution even when used repeatedly. In contrast, a decrease of 23.6% in dye removing capacity of TVFB was noted after five adsorption–desorption cycles. This decrease in the dye removal capacity of TVFB may be related to the loss of TVFB weight (15.69%) during repeated centrifugation. On the other hand, *T. viridi* biomass immobilized in LS discs (TVILS) was stable and only <4.0% decrease in its weight was noted at the end of five consecutive cycles.

3.10. Column studies

3.10.1. Removal of MB by TVILS in fixed-bed column reactors

The performance of biosorbents in continuous dye biosorption process is often an important factor in assessing the feasibility of a biosorbent in real-time practical applications. Therefore, studies were carried out in a fixed-bed packed column to determine the performance of TVILS to remove MB in continuous mode. For this purpose, TVILS discs were packed in a x-scale column bioreactor and 25 mg L^{-1} MB solution was passed through the column in an upward direction at the flow rate of 2.5 mL min^{-1}. The breakthrough biosorption curve is presented in Fig. 12a. The dye loading curve showed an excellent, clear zone (100% removal) before the breakthrough point. The results presented in Fig. 11a show that the column bioreactor packed with TVILS (2.56 ± 0.14 g) had the capacity to treat 12.5 L of 25 mg L^{-1} dye solution before reaching the breakthrough point. The total biosorption capacity of the packed column bioreactor was calculated by integrating the breakthrough curves between the breakthrough and saturation points. The biosorption capacity of the TVILS packed column for 25 mg L^{-1} MB solution was noted to be 205.00 ± 6.08 mg g^{-1}, similar to the maximum value of 201.52 mg g^{-1} obtained during batch-scale studies.

3.10.2. Desorption of MB sorbed on the TVILS in fixed-bed column

Desorption of MB was done with 0.1 M HCl, as mentioned earlier in Section 3.9. The elution breakthrough curve obtained for TVILS discs packed in the fixed-bed column reactor is presented in Fig. 12b. With the elution efficiency of 98.92%, 0.1 M HCl was noted to perform well in the elution of MB from TVILS. It may be noted from the breakthrough curve that MB concentration in the effluent increased sharply during the initial stage, reaching the maximum value (4451 mg L^{-1}) at 90 mL of 0.1 M HCl passed. A gradual decrease in MB concentration was then noted, and the elution process was completed on passing 0.75 L of 0.1 M HCl. The total volume of MB solution treated during the sorption process was 31.5 L, whereas 0.75 L of 0.1 M HCl was used to elute MB during the desorption process. This resulted in a very highly concentrated MB solution elute in very small elutent HCl volume, which was cal-

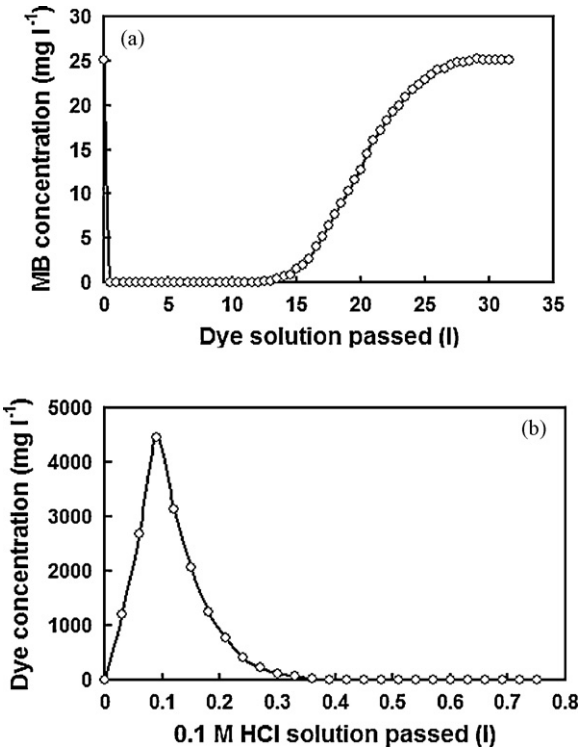

Fig. 12. Biosorption (a) and desorption (b) breakthrough curves for the removal of methylene blue in a fixed-bed column reactor based on immobilized *Trichoderma viride* biomass (TVILS) as the biosorbent in glass column height of 35 cm, internal diameter 2.7 cm, bed pack volume of 30 cm, packed with 2.56 ± 0.14 g immobilized hyphal biomass of *T. viride* (TVILS) at the liquid phase flow rate of 2.5 mL min^{-1} and 0.1 M HCl as the desorption agent.

culated to be 0.4 L. A high concentration factor is preferable as the eventual recovery of dye will become more feasible. In order to assess reusability of the TVILS disc-packed fixed-bed column reactor, a series of adsorption–desorption runs were performed. Like batch studies, the TVILS disc biosorbent, when successively used for adsorption–desorption cycles in fixed-bed columns, retained good dye adsorption capacity even after five repeated cycles. The total decrease in the sorption efficiency of TVILS disc biosorbents after five cycles was only about 2.07%, which shows that TVILS disc biosorbent has good potential to adsorb dye from aqueous solution and can be reused repeatedly. Furthermore, no significant leakage of entrapped biomass or physical damage to TVILS discs was observed during the five repeated adsorption–desorption cycles, as was noted with other polymeric matrices used in immobilized systems resulting in the loss of biosorption capacity of these immobilized systems [14].

4. Conclusions

The study reports on the potential of *T. viride* immobilized onto loofa sponge for the removal of methylene blue from aqueous solution in batch and continuous up-flow fixed-bed packed column operations. TVILS showed good potential for the removal and recovery of MB from aqueous solution at q_{max} of 202 mg g^{-1} in batch studies. No adverse effect on the biosorption capacity of TVILS was observed due to the immobilization matrix of loofa sponge. Additionally, the capacity of TVILS to remove MB, as compared with *T. viride* free biomass, was noted to enhance by 30%. Sorption of MB was dependent on experimental conditions, such as pH, temperature, dye concentration and contact time. Pseudo-second-order kinetics equation and Langmuir adsorption isotherm model were observed to fit to the experimental data. FTIR analysis showed that the main functional sites taking part in the sorption of dye included amine, hydroxyl, carbonyl and amide bonds. TVILS showed good physical and chemical stability as no significant leakage or breakage of immobilized biomass, which accounted for only 3.98% weight loss, was observed during their repeated use in five biosorption–desorption cycles. As much as 99% desorption of MB was achieved with 0.1 M HCl as the elutant. Regenerated TVILS was reused repeatedly during five cycles with only 4.42% loss in its MB uptake capacity, whereas TVFB showed a decrease of 20% in its MB removal capacity, which was possibly due to 15.62% loss in its biomass weight during same number of repeated sorption–desorption cycles. The observations obtained during the present study have clearly indicated the superiority of TVILS over TVFB, and as well as the previously used immobilizing matrices which showed significant decrease in biosorption capacity and release of immobilized biomass during reuse. Loofa sponge is an inexpensive, easily available biomatrix, while immobilization of fungal biomass is easily achieved by simple inoculation procedures without any prior chemical treatments. In contrast, production of immobilized fungal biomass beads using polymeric matrices is expensive and laborious, requiring inputs of sophisticated equipment and procedural protocols. Column experiments have further shown that TVILS can be efficiently used for continuous removal of MB. It may be concluded, therefore, that TVILS has shown the potential of application in the remediation of dye-laden industrial wastewater.

References

[1] X.S. Wang, Y. Zhou, Y. Jiang, C. Sun, The removal of basic dyes from aqueous solutions using agricultural by-products, J. Hazard. Mater. 157 (2008) 374–385.
[2] S.K. Yesiladah, G. Pekin, H. Bermek, I. Arslan-Alation, D. Orhon, C. Tamerler, Bioremediation of textile azo dyes by *Trichophyton rubrum* LSK-27, World J. Microbiol. Biotechnol. 22 (2006) 1027–1031.
[3] R.O.A. de Lima, A.P. Bazo, D.M.F. Salvadori, C.M. Rech, D.P. Oliveira, G.A. Umbuzeiro, Mutagenic and carcinogenic potential of a textile azo dye processing plant effluent that impacts a drinking water source, Mutat. Res. (Genet. Toxicol. Environ. Mutagen.) 626 (2007) 53–60.
[4] G. Crini, Non-conventional low-cost adsorbents for dye removal: a review, Bioresour. Technol. 97 (2006) 1061–1085.
[5] T. Robinson, G. McMullan, R. Marchant, P.R. Nigam, Remediation of dyes in textile effluent: critical review on current treatment technologies with a proposed alternative, Bioresour. Technol. 77 (2001) 247–255.
[6] I.M. Banat, P. Nigam, D. Singh, R. Marchant, Microbial decolorization of textile-dye-containing effluents: a review, Bioresour. Technol. 58 (1996) 217–227.
[7] Z. Aksu, S. Tezer, Biosorption of reactive dyes on the green alga *Chlorella vulgaris*, Process Biochem. 40 (2005) 1347–1361.
[8] T. O'Mahony, E. Guibal, J.M. Tobin, Reactive dye biosorption by *Rhizopus arrhizus* biomass, Enzyme Microb. Technol. 31 (2002) 456–463.
[9] T.L. Hu, Removal of reactive dyes from aqueous solution by different bacterial genera, Water Sci. Technol. 34 (1996) 89–95.
[10] Z. Aksu, G. Domez, A comparative study on the biosorption characteristics of some yeasts for Remazol Blue reactive dye, Chemosphere 50 (2003) 1075–1083.
[11] Y. Fu, T. Viraraghavan, Fungal decolorization of dye wastewaters: a review, Bioresour. Technol. 79 (2001) 251–262.
[12] N.S. Maurya, A.K. Mittal, P. Cornel, E. Rother, Biosorption of dyes using dead macro fungi: effect of dye structure, ionic strength and pH, Bioresour. Technol. 97 (2006) 512–521.
[13] K. Vijayaraghavan, J. Mao, Y.-S. Yun, Biosorption of methylene blue from aqueous solution using free and polysulfone-immobilized *Corynebacterium glutamicum*: Batch and column studies, Bioresour. Technol. 99 (2008) 2864–2871.
[14] K. Vijayaraghavan, M.H. Han, S.C. Choi, Y.-S. Yun, Biosorption of Reactive Black 5 by *Corynebacterium glutamicum* biomass immobilized in alginate and polysulfone matrices, Chemosphere 68 (2007) 1838–1845.
[15] B.-E. Wang, Y.-Y. Hu, L. Xie, K. Peng, Biosorption behavior of azo dye by inactive CMC immobilized *Aspergillus fumigatus* beads, Bioresour. Technol. 99 (2008) 794–800.
[16] K.C. Chen, J.Y. Wu, G.C. Huang, Y.M. Liang, S.C.J. Hwang, Decolorization of azo dye using PVA-immobilized microorganisms, J. Biotechnol. 101 (2003) 241–252.
[17] J.N. Barbotin, J.E. Nava Saucedo, Bioencapsulation of living cells by entrapment in polysaccharide gels, in: Polysaccharides: Structural Diversity and Functional Versatility, Marcel Dekker, New York, 1998, pp. 749–774.
[18] M. Iqbal, A. Saeed, R.G.J. Edyvean, B. O'Sullivan, P. Styring, Production of fungal biomass immobilized loofa sponge (FBILS)-discs for the removal of heavy metal ions and chlorinated compounds from aqueous solution, Biotechnol. Lett. 27 (2005) 1319–1323.
[19] M. Iqbal, A. Saeed, Novel method for cell immobilization and its application for production of organic acid, Lett. Appl. Microbiol. 40 (2005) 178–182.
[20] M. Iqbal, R.G.J. Edyvean, Biosorption of lead, copper and zinc ions on loofa immobilized biomass of *Phanerochaete chrysosporium*, Min. Eng. 17 (2004) 217–223.
[21] M. Iqbal, R.G.J. Edyvean, Loofa sponge immobilized fungal biosorbent: A robust system for cadmium and other dissolved metal removal from aqueous solution, Chemosphere 61 (2005) 510–518.
[22] M. Iqbal, A. Saeed, Biosorption of reactive dye by loofa sponge-immobilized fungal biomass of *Phanerochaete chrysosporium*, Process Biochem. 42 (2007) 1160–1164.
[23] E.N. El Qada, S.J. Allen, G.M. Walker, Adsorption of methylene blue onto activated carbon produced from steam activated bituminous coal: a study of equilibrium adsorption isotherm, Chem. Eng. J. 124 (2006) 103–110.
[24] I. Langmuir, The adsorption of gases on plane surfaces of glass, mica and platinum, J. Am. Chem. Soc. 40 (1918) 1361–1403.
[25] H.M.F. Frenundlich, Über die adsorption in lösungen, Zeitschrift für Physikalische Chemie (Leipzig) 57A (1906) 385–470.
[26] S. Lagergren, Zur theorie der sogenannten adsorption gelöster stoffe, Kungliga Svenska Vetenskapsakademiens, Handlingar 24 (1898) 1–39.
[27] Y.S. Ho, G. McKay, Sorption of dye from aqueous solution by peat, Chem. Eng. J. 70 (1998) 115–124.
[28] M. Minamisawa, H. Minamisawa, S. Yoshida, N. Takai, Adsorption of heavy metals on biomaterials, J. Agric. Food Chem. 52 (2004) 5606–5611.
[29] G. Bayramoglu, G. Celik, Y. Arica, Biosorption of Reactive Blue 4 dye by native and treated fungus *Phanerochaete chrysosporium*: batch and continuous flow system studies, J. Hazard. Mater. B137 (2006) 1689–1697.
[30] M.Y. Arica, G. Bayramoglu, Biosorption of Reactive Red 120 dye from aqueous solution by native and modified fungus biomass preparations of *Lentinus sajor-caju*, J. Hazard. Mater. 149 (2007) 499–507.
[31] A. Kapoor, T. Viraraghavan, Heavy metal biosorption sites in *Aspergillus niger*, Bioresour. Technol. 61 (1997) 221–227.
[32] D. Penman, G. Britton, K. Hardwick, H.A. Collin, S. Isaac, Chitin as a measure of biomass of *Crinipellis perniciosa*, causal agent of witches' broom disease of *Theobroma cacao*, Mycol. Res. 104 (2000) 671–675.
[33] R. Dolphen, N. Sakkayaawong, P. Thiravetyan, W. Nakbanpote, Adsorption of Reactive Red 141 from wastewater onto modified chitin, J. Hazard. Mater. 145 (2007) 250–255.
[34] S.I. Zafar, M. Bisma, A. Saeed, M. Iqbal, FTIR spectrophotometry, kinetics and adsorption isotherms modeling, and SEM-EDX analysis for describing mechanism of biosorption of the cationic basic dye methylene blue by a new biosorbent (sawdust of silver fir; *Abies pindrow*), Fresenius Environ. Bull. 17 (2008) 2109–2121.

[35] M.C. Ncibi, B. Mahjoub, M. Seffen, Kinetic and equilibrium studies of methylene blue biosorption by *Posidonia oceanica* (L) fibers, J. Hazard. Mater. B139 (2007) 280–285.
[36] Z. Aksu, Application of biosorption for the removal of organic pollutants: a review, Process Biochem. 40 (2005) 997–1026.
[37] K. Vijayaraghavan, S.W. Won, J. Mao, Y.-S. Yun, Chemical modification of *Corynebacterium glutamicum* to improve methylene blue biosorption, Chem. Eng. J. 145 (2008) 1–6.
[38] S. Cengiz, L. Cavas, Removal of methylene blue by invasive marine seaweed: *Caulerpa racemosa* var. *cylindracea*, Bioresour. Technol. 99 (2008) 2357–2363.
[39] B.H. Hameed, D.K. Mahmoud, A.L. Ahmad, Sorption of basic dye from aqueous solution by pomelo (*Citrus grandis*) peel in a batch system, Colloids Surf. A: Physicochem. Eng. Aspects 316 (2008) 78–84.
[40] C. Nainasivayam, K. Kadirvelu, Coir pith, an agricultural waste by-product for the treatment of dying wastewater, Bioresour. Technol. 48 (1994) 79–81.
[41] K. Vijayaraghavan, J. Mao, Y.-S. Yun, Biosorption of methylene blue from aqueous solution using free and polysulfone-immobilized *Corynebacterium glutamicum*: batch and column studies, Bioresour. Technol. 99 (2008) 2864–2871.
[42] N. Kannan, M.M. Sundaram, Kinetics and mechanism of removal of methylene blue by adsorption on various carbon: a comparative study, Dyes Pigments 51 (2001) 25–40.
[43] Z. Aksu, A.I. Tatli, O. Tunc, A comparative adsorption/biosorption study of Acid Blue 161: effect of temperature on equilibrium and kinetic parameters, Chem. Eng. J. 142 (2008) 23–39.
[44] Z. Aksu, S. Tezer, Equilibrium and kinetic modelling of biosorption of Remazol Black B by *Rhizopus arrhizus* in a batch system: effect of temperature, Process Biochem. 36 (2000) 431–439.
[45] Y. Ting, G. Sun, Use of polyvinyl alcohol as a cell immobilization matrix for copper biosorption by yeast cells, J. Chem. Technol. Biotechnol. 75 (2000) 541–546.
[46] R. Gourdon, E. Rus, S. Bhende, S.S. Sofer, A comparative study of cadmium uptake by free and immobilized cells from activated sludge, J. Environ. Sci. Health A25 (1990) 1019–1036.
[47] M.S. Alhakawasti, C.J. Banks, Removal of copper from aqueous solution by *Ascophyllum nodosum* immobilised in hydrophilic polyurethane foam, J. Environ. Manage. 72 (2004) 195–204.
[48] V.J.P. Vilar, C.M.B. Botelho, R.A.R. Boaventura, Methylene blue adsorption by algal biomass based materials: biosorbents characterization and process behaviour, J. Hazard. Mater. 147 (2007) 120–132.
[49] M.Y. Arıca, G. Bayramoglu, M. Yılmaz, S. Bektas, O. Genç, Biosorption of Hg^{2+}, Cd^{2+}, and Zn^{2+} by Ca-alginate and immobilized wood-rotting fungus *Funalia trogii*, J. Hazard. Mater. B109 (2004) 191–199.
[50] R.S. Prakasham, J.S. Merrie, R. Sheela, N. Saswathi, S.V. Ramakrishna, Biosorption of chromium VI by free and immobilized *Rhizopus arrhizus*, Environ. Poll. 104 (1999) 421–427.
[51] K.R. Hall, L.C. Eagleton, A. Acrivos, T. Vermeulen, Pore- and solid-diffusion kinetics in fixed bed adsorption under constant-pattern conditions, Ind. Eng. Chem. Fund. 5 (1996) 212–223.
[52] T.W. Weber, P.K. Chakravorti, Pore and solid diffusion models for fixed adsorbers, AIChE J. 20 (1974) 226–237.
[53] F.A. Pavan, E.C. Lima, S.L.P. Dias, A.C. Mazzocato, Methylene blue biosorption from aqueous solutions by yellow passion fruit waste, J. Hazard. Mater. 150 (2008) 703–712.
[54] V.J.P. Vilar, C.M.S. Botelho, R.A.R. Boaventura, Methylene blue adsorption by algal biomass based materials: Biosorbents characterization and process behaviour, J. Hazard. Mater. 147 (2007) 120–132.
[55] S. Wang, T. Terdkiatburana, M.O. Tade, Single and co-adsorption of heavy metals and humic acid on fly ash, Sep. Purif. Technol. 58 (2008) 353–358.
[56] J.C.P. Vaghetti, E.C. Lima, B. Royer, J.L. Brasil, B.M. da Cunha, N.M. Simon, N.F. Cardoso, C.P.Z. Norena, Application of Brazilian-pine fruit coat as a biosorbent to removal of Cr(VI) from aqueous solution: Kinetics and equilibrium study, Biochem. Eng. J. 42 (2008) 67–76.
[57] V. Lugo-Lugo, S. Hernandez-Lopez, C. Barrera-Diaz, F. Urena-Nunez, B. Bilyeu, A comparative study of natural, formaldehyde-treated and copolymer-grafted orange peel for Pb(II) adsorption under batch and continuous mode, J. Hazard. Mater. 161 (2009) 1255–1264.
[58] D.L. Sparks, Soil Physical Chemistry, second ed., CRC Press, USA, 1999.